Research article

Yuhao Guo, Jing Wang, Zhaohong Han, Kazumi Wada, Lionel C. Kimerling, Anuradha M. Agarwal, Jurgen Michel, Zheng Zheng, Guifang Li and Lin Zhang*

Power-efficient generation of two-octave mid-IR frequency combs in a germanium microresonator

https://doi.org/10.1515/nanoph-2017-0131
Received December 21, 2017; revised April 27, 2018; accepted May 14, 2018

Abstract: Octave-spanning frequency comb generation in the deep mid-infrared (>5.5 μm) typically requires a high pump power, which is challenging because of the limited power of narrow linewidth lasers at long wavelengths. We propose twofold dispersion engineering for a Ge-on-Si microcavity to enable both dispersion flattening and dispersion hybridization over a wide band from 3.5 to 10 μm. A two-octave mode-locked Kerr frequency comb can be generated from 2.3 to 10.2 μm, with a pump power as low as 180 mW. It has been shown that dispersion flattening greatly enhances the spectral broadening of the generated comb, whereas dispersion hybridization improves its spectral flatness.

Keywords: nonlinear optics; integrated optics devices; mid-infrared; dispersion engineering; optical frequency comb.

1 Introduction

Recently, frequency comb generation in the mid-infrared (mid-IR) has become an intensely investigated topic for spectroscopy and imaging applications [1]. Kerr frequency combs generated in mid-IR microresonators [2–5] can be compact and broadband, suitable for building a portable device [6–9]. Many of the optical materials used thus far for mid-IR photonics become strongly absorptive above 5.5 μm wavelength, whereas the term "mid-IR" means a large spectral range, from 2.5 to 20 μm, i.e. three octaves [10–13], with many molecular fingerprints to be detected. Some material combinations, e.g. chalcogenide glasses and Ge/Si, can be used as waveguide core and cladding at more than 5.5 μm in the deep mid-IR. However, thermal effect becomes more severe, and chalcogenides might suffer from this due to their relatively low thermal conductivity and glass transition temperature. Ge-on-Si waveguides and microresonators would be desirable [10, 11, 14, 15], as Ge has a high refractive index (~4.3), strong nonlinearity, no two- and three-photon absorptions above 5 μm, and CMOS compatibility.

There are few technical challenges for wideband mode-locked Kerr comb generation in the deep mid-IR. If the higher-order (>2) dispersions and other nonlinear effects such as self-steepening and Raman scattering are ignored, cavity-soliton-based mode-locked combs have their bandwidth related to the following physical parameters [16]:

$$\Delta f_{3\mathrm{dB}} \propto \sqrt{\frac{\gamma PF}{|\beta_2|}} \tag{1}$$

***Corresponding author: Lin Zhang,** Key Laboratory of Opto-electronic Information Technical Science of Ministry of Education, School of Precision Instruments and Opto-electronics Engineering, Tianjin University, Tianjin 300072, China; Key Laboratory of Integrated Opto-electronic Technologies and Devices in Tianjin, School of Precision Instruments and Opto-electronics Engineering, Tianjin University, Tianjin 300072, China; and Department of Materials Science and Engineering, Massachusetts Institute of Technology, Cambridge, MA 02139, USA, e-mail: lin_zhang@tju.edu.cn.
http://orcid.org/0000-0003-0545-1110
Yuhao Guo and Jing Wang: Key Laboratory of Opto-electronic Information Technical Science of Ministry of Education, School of Precision Instruments and Opto-electronics Engineering, Tianjin University, Tianjin 300072, China; and Key Laboratory of Integrated Opto-electronic Technologies and Devices in Tianjin, School of Precision Instruments and Opto-electronics Engineering, Tianjin University, Tianjin 300072, China
Zhaohong Han, Lionel C. Kimerling, Anuradha M. Agarwal and Jurgen Michel: Department of Materials Science and Engineering, Massachusetts Institute of Technology, Cambridge, MA 02139, USA
Kazumi Wada: Department of Materials Engineering, University of Tokyo, Tokyo 113-8656, Japan
Zheng Zheng: School of Electronic and Information Engineering, Beihang University, Beijing 100191, China; and Collaborative Innovation Center of Geospatial Technology, Wuhan 430079, China
Guifang Li: Key Laboratory of Opto-electronic Information Technical Science of Ministry of Education, School of Precision Instruments and Opto-electronics Engineering, Tianjin University, Tianjin 300072, China; Key Laboratory of Integrated Opto-electronic Technologies and Devices in Tianjin, School of Precision Instruments and Opto-electronics Engineering, Tianjin University, Tianjin 300072, China; and College of Optics and Photonics, CREOL and FPCE, University of Central Florida, Orlando, FL 32816, USA

where the nonlinear coefficient γ is nearly inversely proportional to λ^3 [γ is expressed as $2\pi n_2/(A_{\text{eff}}\lambda)$, where n_2 is the nonlinear index of the refraction of the guided mode, which has little change over the spectra where four-photon absorption can be negligible, and A_{eff} is the effective mode area, which is almost proportional to λ^2] and dramatically decreases with wavelength; the cavity finesse F is mostly determined by the Q factor, which is limited by a high scattering loss in high-index cavities due to sidewall roughness; the pump power P is also limited by narrow-linewidth quantum cascaded lasers associated with thermal problem in the mid-IR; and β_2 is the group-velocity dispersion. Due to the rapidly decreasing nonlinear coefficient, loss-induced low finesse, and limited availability of high-power lasers and amplifiers, there have been few reports on mid-IR microresonator-based comb generation above 5.5 μm. Dispersion engineering is believed to be the key to achieve a wideband mode-locked Kerr comb with a limited pump power.

Here, we present twofold efforts in dispersion engineering to solve the above problem: (i) dispersion flattening and (ii) dispersion hybridization. First, it is desirable to obtain low and flat dispersion over a wide band where near-zero dispersion is maintained [17, 18] for an octave-spanning comb. However, the previously proposed dispersion flattening technique [17, 18] requires using a low-index material (e.g. SiO_2) to form a slot structure that is not practically more than 5 μm because of high material absorption. Second, even with a flattened anomalous dispersion, widely apart comb lines will still see a large group delay difference over an octave-spanning bandwidth, making it difficult to achieve a wide comb spectrum associated with an ultra-short cavity soliton. Thus, it is worth exploring a new comb generation mechanism with normal dispersion introduced into a dispersion profile, which can further reduce the group delay difference between the widely apart frequency components and contribute to the generation of a dispersive wave that broadens the soliton spectrum. However, this is controversial to an established rule that a bright soliton needs anomalous dispersion over its whole spectrum in general.

In this work, we propose a Ge-on-Si microresonator for power-efficient frequency comb generation in the deep mid-IR, which is dispersion flattened without using a slot. The cavity is designed by jointly considering dispersion, single modeness, effective mode volume, and different loss mechanisms. In particular, we hybridize the dispersion profile with a normal dispersion in the middle, between two anomalous dispersion bands, which is called the hybrid dispersion here. As a result, a two-octave Kerr comb can be generated in the deep mid-IR from 2.3 to 10.2 μm with the pump power reduced to only 180 mW. Intriguingly, this comb can be mode locked via bright cavity soliton formation, even with this hybrid dispersion, which is studied for the first time as an effective way to reduce pump power requirement.

2 Resonator configuration

Figure 1 shows a Ge waveguide on the Si-on-insulator platform, and the buried SiO_2 layer is partially etched to avoid a strong material absorption above 3.8 μm [11], leaving an Si slab to support the Ge waveguide. The structural parameters of this waveguide are width = 880 nm, Ge height = 2200 nm, Si ridge height = 600 nm, Si slab height = 530 nm, and sidewall angle = 87°. In the design of this waveguide, several issues have to be taken into account simultaneously.

First, dispersion flattening without using a slot is different from previous dispersion engineering schemes [17, 18]. Here, we control the optical mode extension from Ge to Si as the wavelength increases, which determines the effective refractive index as a function of wavelength [19]. In Ref. [19], the material indices are relatively small, but in this work Ge has a very high index contrast with air, which causes a strong waveguide dispersion. Thus, we change the low-index part (i.e. Si part) from a strip as in Ref. [19] to a ridge/slab structure in Figure 1 for dispersion engineering, and the slab also serves to support the whole waveguide. In principle, the role of the Si part is to allow the mode to extend to Si instead of air so that one can tailor the Si ridge dimensions to control the mode extension and the effective index. We

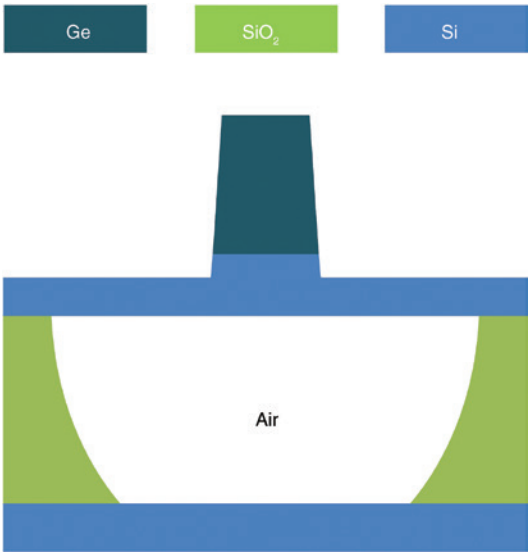

Figure 1: Cross-section of the CMOS-compatible dispersion-flattened Ge-on-Si waveguide with SiO_2 substrate partially removed.

use the fundamental quasi-TM mode, and a full-vectorial finite-element method is employed for mode analysis. All material dispersions are taken into account using the Sellmeier equations [11]. As shown in Figure 2A, an ultra-low and flat dispersion is obtained from 3.5 to 10 μm. Note that the dispersion is hybrid, which has both normal and anomalous dispersions over the above bandwidth, with a variation from –16 to 32 ps/nm/km, and the zero-dispersion wavelengths (ZDWs) are located at 3.315, 5.645, 7.405, and 9.708 μm, respectively. γ is also calculated over wavelength with the nonlinear index n_2 in [11], which decreases quickly in Figure 2A.

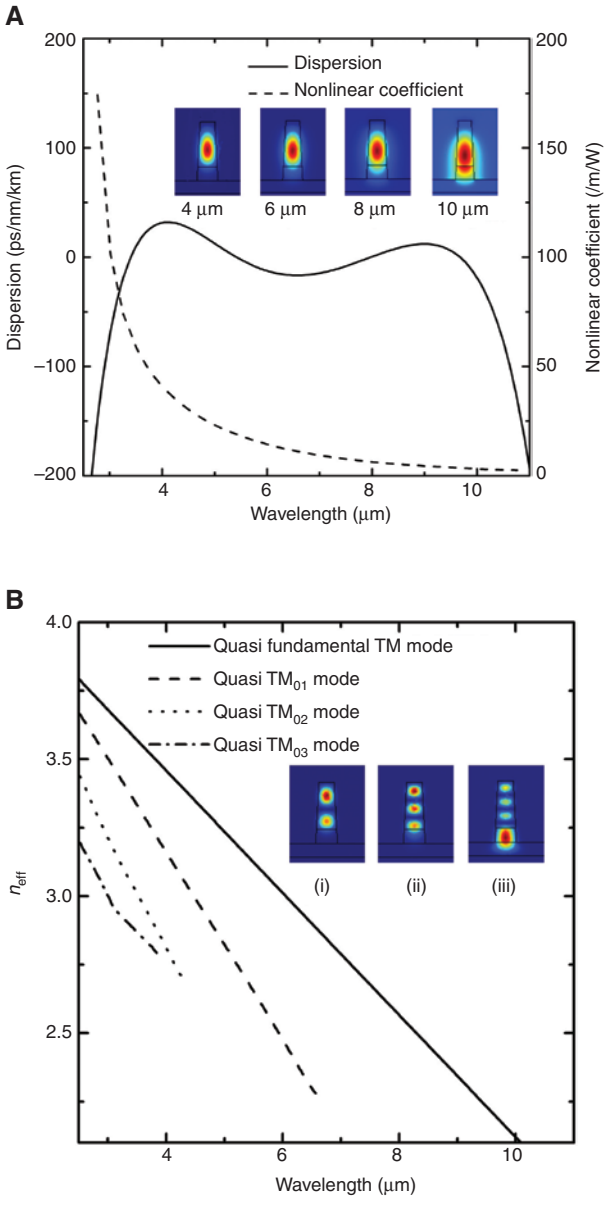

Figure 2: Dispersion, nonlinearity, and mode behaviors of the proposed waveguide.
(A) A flattened and hybrid dispersion profile (solid) and the nonlinear coefficient (dashed) over a wide wavelength range in the mid-IR. Insets: Mode field distributions of the fundamental quasi-TM mode at 4, 6, 8, and 10 μm wavelengths. (B) Effective indices of higher-order TM modes versus wavelength.

Second, the higher-order modes need to be suppressed as much as possible. In fact, as we pursue octave-spanning comb generation, even if a waveguide is designed to be single mode on the long-wavelength side, it naturally becomes a multimode waveguide on the other side, where the wavelength is almost halved. Thus, the suppression of the higher-order modes should be taken into consideration while tailoring the dispersion of the waveguide. We design a quite small waveguide width here instead of reducing the waveguide height. In this way, we can reduce the number of the higher-order modes without increasing the substrate leakage much. Figure 2B presents the mode characteristics of this waveguide. There are three higher-order modes at the TM polarization that are adjacent to the fundamental TM mode, i.e. TM_{01}, TM_{02}, and TM_{03} modes, respectively. The effective indices of the three modes change with wavelength at different rates, and their cutoff wavelengths are all below the central wavelength (6.6 μm) of the flat dispersion band in Figure 2A.

Third, the optical losses of the designed waveguide mainly include material absorption, substrate leakage, and scattering loss. The material losses in Si and Ge are shown in Figure 3A [11]. Ge is quite transparent, whereas Si becomes lossy above 8.5 μm. As we use Si as bottom cladding, it does not add much to the total loss as confirmed by the comparison in Figure 3B. Regarding substrate leakage, light is confined well in the core and almost no field leaks into the substrate at short wavelengths. As wavelength increases, the mode field spreads more into the Si substrate. If no material absorption is taken into the model, the substrate leakage becomes severe above 11 μm (dashed line) in Figure 3B. After adding the material losses, we find a slightly increased loss (solid line) in Figure 3B. The scattering loss is not easy to be calculated. Here, we assume the scattering loss to be 3 dB/cm because of a relatively small width used compared to the waveguide with a scattering loss of 2.5 dB/cm measured in Ref. [14].

To realize frequency comb generation in a Ge microresonator, which is based on the proposed waveguide, we have to balance between a small mode volume and a high bending loss. Based on a cylindrical coordinate system [20, 21], we calculate the bending loss versus wavelength for different ring radii: 12, 15, 18, and 20 μm, respectively. As shown in Figure 3C, the bending loss increases significantly above 7 μm for a radius of 12 μm. Moreover, the bending loss decreases dramatically as the radius increased.

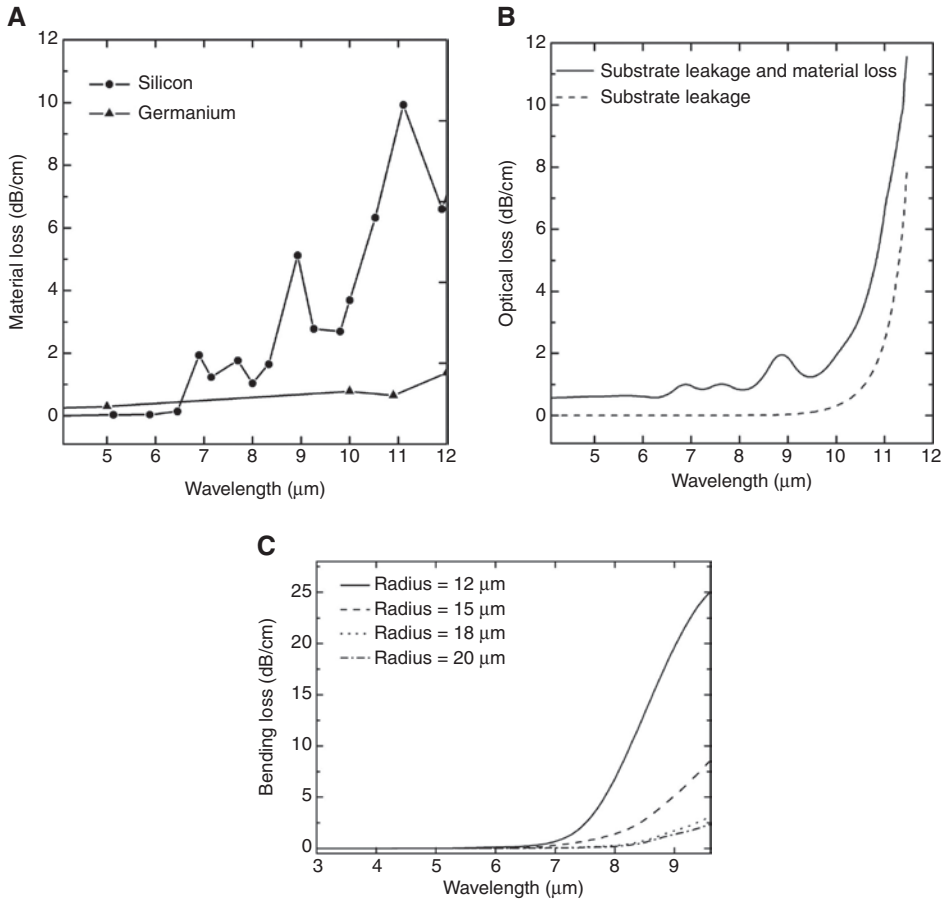

Figure 3: Loss properties of the proposed devices.
(A) Material losses of Si and Ge; (B) substrate leakage of the quasi-TM mode dramatically increases with wavelength above 11 μm (dashed line), and material losses of Si and Ge do not add much (solid line); and (C) bending loss versus wavelength in the Ge ring resonator for different bending radii: 12, 15, 18, and 20 μm.

3 Comb generation

We use a microresonator with a bending radius of 12 μm for frequency comb generation. With optical losses above, we obtain a Q factor of 40,000 at 4.51 μm wavelength. The free spectral range is 1 THz, and accordingly, the finesse is about 600. We use the Lugiato-Lefever equation [6, 16, 22] to simulate the comb generation with a temporal step of 1 fs. We pump the microresonator at the resonance adjacent to 4.51 μm in the anomalous dispersion band, and the pump power is 180 mW, which is available from the state-of-the-art quantum cascaded lasers. The comb generation process is seen in Figure 4, as shown by the spectral and temporal snapshots at the normalized pump detuning $\Delta = 0$, 4, and 10, and Δ is defined as $2\delta_0/(\alpha + \kappa)$, where δ_0 is the phase detuning of the pump from the closest cavity resonance, α is the internal linear roundtrip loss of the cavity, and κ is the input coupler power transmission coefficient, as described in Ref. [16]. κ here is 5.188×10^{-3}. The comb spectrum becomes increasingly smooth, and accordingly, the intracavity field evolves into a pulsed waveform, as a result of a transition of the generated comb from the modulational instability regime to the cavity soliton regime [23, 24], as presented by Figure 4B. Finally, a single bright soliton is formed with a full-width at half-maximum of 16 fs (i.e. single-cycle level) and a peak power of 63 W, corresponding to a two-octave mode-locked frequency comb from 2.3 to 10.2 μm at –30 dB level. A strong dispersive wave is found at 2.41 μm. The generated comb has a nonlinear conversion efficiency of 4.1% [25].

It is important to note that the bright soliton's spectrum fully covers the two anomalous dispersion bands and the normal dispersion band in the middle, which is smooth and mode locked. This can be explained as follows. As the comb spectrum is very wide, where dispersion varies with wavelength, the overall dispersion experienced by the whole comb is still anomalous. Thus, one can expect a bright soliton.

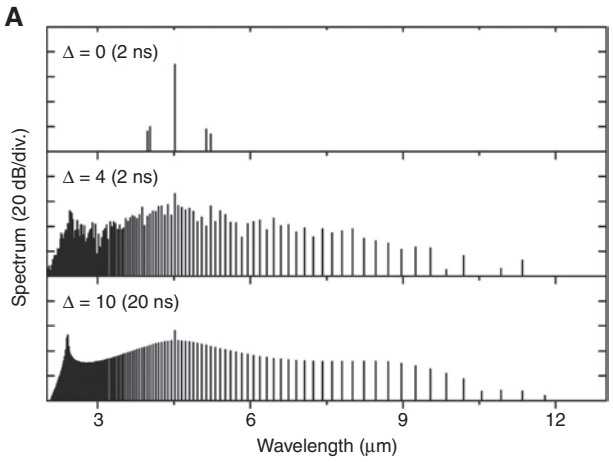

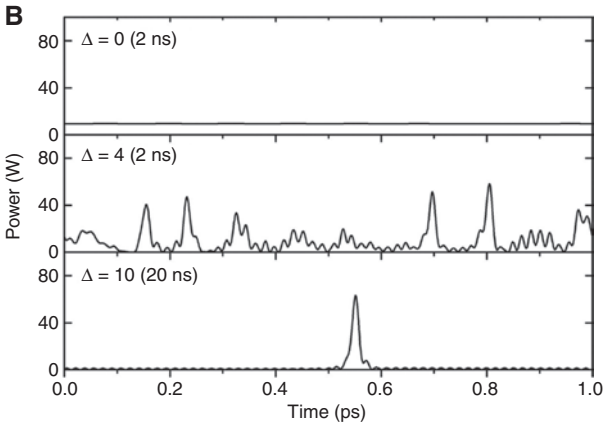

Figure 4: Comb generation in (A) frequency and (B) time domains at the normalized pump detuning $\Delta = 0$, 4, and 10.
A Kerr frequency comb is generated by a 180 mW CW pump at 4.51 μm, and the comb is mode locked via soliton formation.

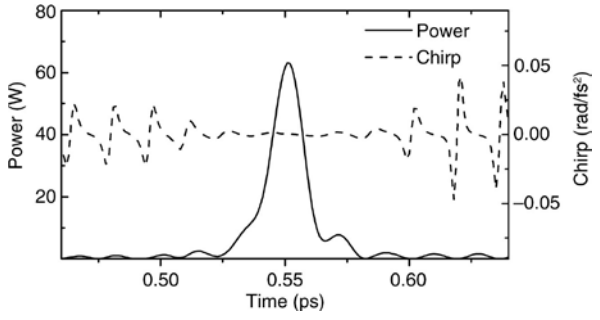

Figure 5: Pulse waveform (solid line) and its frequency chirp (dashed line) in the time domain.
The main pulse is slightly chirped.

We also show the pulse waveform (solid curve) and frequency chirp (dashed curve) in the time domain in Figure 5. The soliton is slightly chirped at the pulse peak, and the chirp is about 1.5×10^{-4} rad/fs^2, which can be caused by the unusual dispersion profile mentioned above, Raman scattering, self-steepening, and especially the generation of dispersive waves.

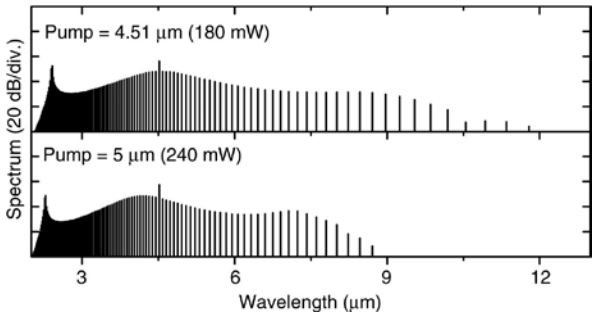

Figure 6: Pump wavelength is shifted from 4.51 to 5 μm, respectively.
When the pump is at a long wavelength, the pump power has to be increased due to a small nonlinear coefficient.

According to the dispersion profile in Figure 2A, we see that there is a low dispersion band from 3.5 to 10 μm wavelength, and one can tune the pump wavelength based on the availability of pump lasers. For comparison, we keep the $X = 10$ (X is defined in Ref. [16]), indicating the same normalized pump power. Due to a rapid decrement of the nonlinear coefficient as wavelength increases, as seen in Figure 2A, the actual pump power changes accordingly. Figure 6 shows the generated comb spectra, and we see that the comb can be mode locked, when pumped at 4.51 and 5 μm, showing a certain flexibility of choosing the pumping wavelength. Note that, when pumping at 4.51 μm, we only need a pump power of 180 mW for a Kerr comb from 2.3 to 10.2 μm. In contrast, one needs a pump power of 240 mW, when pumping at 5 μm, and the comb bandwidth is from 2.5 to 8.1 μm, as shown in Figure 6.

We then examine comb generation for a different bending radius with the same pump power of 180 mW at 4.51 μm, as shown in Figure 7. The comb bandwidth is almost independent of the radius. Although the comb spectrum for a 12 μm radius has a slightly higher comb line power of about 6 μm due to an increased mode volume in the nonlinear cavity, the bending radius of 20 μm might be preferred for more comb lines above 9 μm wavelength.

To more clearly show the benefit of the proposed twofold dispersion engineering, we present three comb spectra in Figure 8, each corresponding to a cavity with specific parameter combination. Cavity 1 has the parameters mentioned above, generating a hybrid dispersion with four ZDWs. Cavity 2 (another Ge-on-Si cavity) generates an anomalous dispersion from 3.36 to 10.42 μm with two ZDWs. Cavity 3 is a low dispersion Ge strip cavity reported in Ref. [11]. Their dispersion curves are shown in Figure 8A. Cavities 1 and 2 produce a saddle-shaped

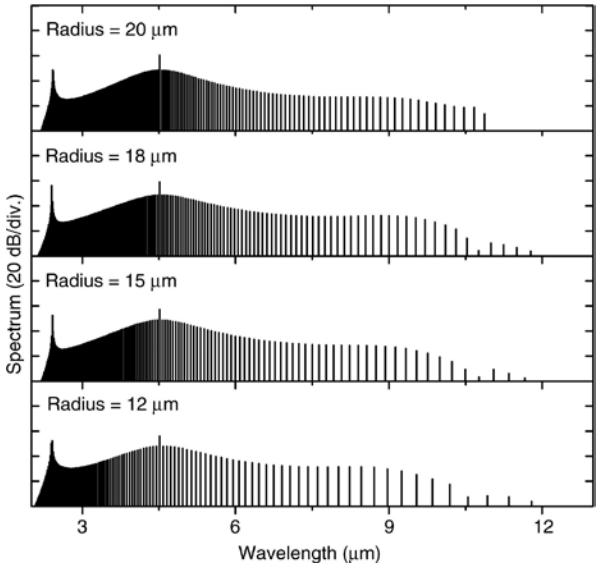

Figure 7: Frequency comb generation at different bending radii with the same pump power.

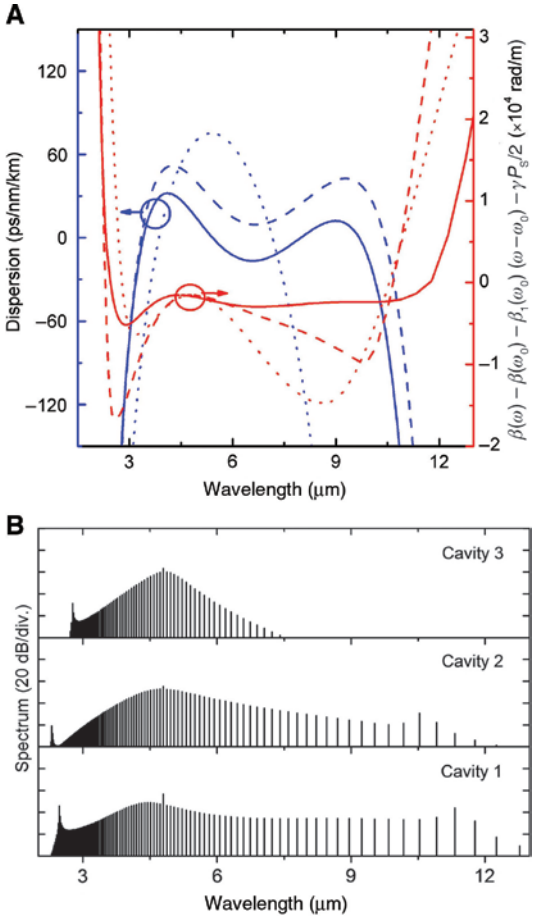

Figure 8: Frequency comb generation in three cavities.
(A) Dispersion curves for cavity 1 (solid line), cavity 2 (dashed line), and cavity 3 (dotted line) and (B) generated frequency comb spectra for cavities 1 to 3, with a pump power of 300 mW at 4.8 μm.

dispersion profile via dispersion flattening, which effectively reduces the dispersion value experienced by the main part of the generated combs. We use a pump wavelength at 4.8 μm and a pump power of 300 mW. The comb bandwidths for cavities 1 to 3 are 9.4, 6.1, and 2.5 μm, respectively, at –30 dB level, as shown in Figure 8B. All-order dispersions are considered here, and the phase-matching parameter, defined as $\beta(\omega)-\beta(\omega_0)-\beta_1(\omega_0)(\omega-\omega_0)-\gamma P_s/2$, where P_s is the soliton peak power [26], for three cavities is shown in Figure 8A, predicting the locations of dispersive waves in good agreement with those in Figure 8B. It is important to note that, in contrast to the cavities 2 and 3 cases, for cavity 1, the peak of the comb spectrum is blue shifted, away from the pump wavelength, where dispersion is more anomalous. Thus, when the phase-matching parameter is calculated, ω_0 should be the peak angular frequency of the comb spectrum, which may not be exactly the angular frequency of the pump.

First, the impact of dispersion flattening is shown by comparing the generated combs using cavities 2 and 3. Dramatically extended dispersion bandwidth and reduced dispersion value in cavity 2 support comb spectrum broadening to the deep mid-IR range up to 12 μm. Second, dispersion hybridization greatly contributes to the frequency comb improvement due to the generation of a dispersive wave at longer wavelengths compared to cavity 2. The comb spectrum from cavity 1 becomes much flatter, from 6 to 11 μm, compared to that from cavity 2. In particular, the comb line power varies by only –3 dB over a wide spectral range from 6.3 to 8.7 μm, which reveals a highly desired power transfer from the pump to distant comb lines.

4 Summary

We have presented a dispersion-flattened Ge-on-Si microcavity for power-efficient generation of two-octave frequency combs in the mid-IR. A flattened and hybrid dispersion is achieved from 3.5 to 10 μm as a key enabler for comb spectral broadening and pump power reduction. Based on this unique dispersion, we showed that a mode-locked Kerr frequency comb could be generated from 2.3 to 10.2 μm with only 180 mW pump power required.

Acknowledgments: This work was supported in part by the National Basic Research Program of China (973) Project #2014CB340104/3, NSFC Projects 61775164, 61335005, 61575142, and 61431009. We also acknowledge the support from the Advanced Integrated Optoelectronics Facility at the Tianjin University.

References

[1] Schliesser A, Picqué N, Hänsch TW. Mid-infrared frequency combs. Nat Photonics 2012;6:440–9.

[2] Wang CY, Herr T, Del'Haye P, et al. Mid-infrared optical frequency combs at 2.5 μm based on crystalline microresonators. Nat Commun 2013;4:1345.

[3] Griffith AG, Lau RKW, Cardenas J, et al. Silicon-chip mid-infrared frequency comb generation. Nat Commun 2015;6:6299.

[4] Savchenkov AA, Ilchenko VS, Di Teodoro F, et al. Generation of Kerr combs centered at 4.5 μm in crystalline microresonators pumped with quantum-cascade lasers. Opt Lett 2015;40:3468–71.

[5] Yu M, Okawachi Y, Griffith AG, Lipson M, Gaeta AL. Mode-locked mid-infrared frequency combs in a silicon microresonator. Optica 2016;3:854–60.

[6] Chembo YK, Menyuk CR. Spatiotemporal Lugiato-Lefever formalism for Kerr-comb generation in whispering-gallery-mode resonators. Phys Rev A 2013;87:053852.

[7] Huang SW, Yang J, Yu M, et al. A broadband chip-scale optical frequency synthesizer at 2.7×10^{-16} relative uncertainty. Sci Adv 2016;2:e1501489.

[8] Hansson T, Wabnitz S. Bichromatically pumped microresonator frequency combs. Phys Rev A 2014;90:013811.

[9] Xue X, Xuan Y, Liu Y, et al. Mode-locked dark pulse Kerr combs in normal-dispersion microresonators. Nat Photonics 2015;9:594–600.

[10] Soref R. Mid-infrared photonics in silicon and germanium. Nat Photonics 2010;4:495–7.

[11] Zhang L, Agarwal AM, Kimerling LC, Michel J. Nonlinear group IV photonics based on silicon and germanium: from near-infrared to mid-infrared. Nanophotonics 2014;3:247–68.

[12] Petersen R, Moller U, Kubat I, et al. Mid-infrared supercontinuum covering the 1.4–13.3 μm molecular fingerprint region using ultra-high NA chalcogenide step-index fibre. Nat Photonics 2014;8:830–4.

[13] Zhao Z, Wu B, Wang X, et al. Mid-infrared supercontinuum covering 2.0–16 μm in a low-loss telluride single-mode fiber. Laser Photon Rev 2017;11:1700005.

[14] Chang YC, Paeder V, Hvozdara L, Hartmann JM, Herzig HP. Low-loss germanium strip waveguides on silicon for the mid-infrared. Opt Lett 2012;37:2883–5.

[15] Yuan J, Kang Z, Li F, et al. Mid-infrared octave-spanning supercontinuum and frequency comb generation in a suspended germanium-membrane ridge waveguide. J Lightwave Technol 2017;35:2994–3002.

[16] Coen S, Erkintalo M. Universal scaling laws of Kerr frequency combs. Opt Lett 2013;38:1790–2.

[17] Zhang L, Yue Y, Beausoleil RG, Willner AE. Flattened dispersion in silicon slot waveguides. Opt Express 2010;18:20529–34.

[18] Zhang L, Mu J, Singh V, Agarwal AM, Kimerling LC, Michel J. Intra-cavity dispersion of microresonators and its engineering for octave-spanning Kerr frequency comb generation. IEEE J Sel Top Quantum Electron 2014;20:5900207.

[19] Guo Y, Jafari Z, Agarwal AM, et al. Bilayer dispersion-flattened waveguides with four zero-dispersion wavelengths. Opt Lett 2016;41:4939–42.

[20] Lui W, Xu C, Hirono T, Yokoyama K, Huang W. Full-vectorial wave propagation in semiconductor optical bending waveguides and equivalent straight waveguide approximations. J Lightwave Technol 1998;16:910–4.

[21] Kakihara K, Kono N, Saitoh K, Koshiba M. Full-vectorial finite element method in a cylindrical coordinate system for loss analysis of photonic wire bends. Opt Express 2006;14:11128–41.

[22] Zhang L, Bao C, Singh V, et al. Generation of two-cycle pulses and octave-spanning frequency combs in a dispersion-flattened micro-resonator. Opt Lett 2013;38:5122–5.

[23] Herr T, Brasch V, Jost JD, et al. Temporal solitons in optical microresonators. Nat Photonics 2014;8:145–52.

[24] Lamont MRE, Okawachi Y, Gaeta AL. Route to stabilized ultrabroadband microresonator-based frequency combs. Opt Lett 2013;38:3478–81.

[25] Bao C, Zhang L, Matsko A, et al. Nonlinear conversion efficiency in Kerr frequency comb generation. Opt Lett 2014;39:6126–9.

[26] Bao C, Taheri H, Zhang L, et al. High-order dispersion in Kerr comb oscillators. J Opt Soc Am B 2017;34:715–25.